Nanoscale and Microscale Thermophysical Engineering, 19: 166–182, 2015

ISSN: 1556-7265 print / 1556-7273 online
DOI: 10.1080/15567265.2015.1035199

Taylor & Francis
Taylor & Francis Group

PHONON DYNAMICS AT SURFACES AND INTERFACES AND ITS IMPLICATIONS IN ENERGY TRANSPORT IN NANOSTRUCTURED MATERIALS—AN OPINION PAPER

Deyu Li[1] and Alan J. H. McGaughey[2]

[1]*Department of Mechanical Engineering, Vanderbilt University, Nashville, Tennessee, USA*

[2]*Department of Mechanical Engineering, Carnegie Mellon University, Pittsburgh, Pennsylvania, USA*

Nanoscale thermal transport has attracted considerable attention because of both fundamental scientific interest and important engineering applications. For semiconductors and insulators, energy transport is dominated by phonons, whose behavior at surfaces and interfaces plays a significant role in energy transport processes. In this article, we present opinions on phonon dynamics at surfaces and interfaces and the implications on nanoscale thermal transport. The effects of roughness, bonding strength, coherence, and nanoscale constrictions are discussed. The existence of two specularity parameters at an interface (separate values for transmitted and reflected phonons) and the implications of phonon reflection at free surfaces to the thermal conductance of nearby interfaces are two concepts that have not been previously discussed in the literature. We provide some outlook and potential topics for future studies.

KEY WORDS: phonon transport, surfaces, interfaces, phonon coherence

INTRODUCTION

The thermal transport properties of nanostructured materials are important in many potential applications, including thermal management of micro/nanoelectronic devices, photovoltaic and thermoelectric energy conversion, and design of nanocomposites with desirable properties [1, 2]. For semiconductors and insulators, lattice vibrations (i.e., phonons) are responsible for thermal transport. Given that individual nanostructures and nanostructured materials have extremely large surface/interface area–to-volume ratios, the behavior of phonons at boundaries (i.e., surfaces and interfaces) plays a critical role in their thermal transport properties. These effects are being intensively studied because a better understanding of phonon dynamics at surfaces and interfaces could lead to faster nanoelectronic devices [3], more efficient energy converters [4], and composite materials with tunable thermal conductivities [5].

Manuscript received 3 November 2014; accepted 25 March 2015.

Address correspondence to Deyu Li, Department of Mechanical Engineering, VU Station B#351592, Vanderbilt University, Nashville, TN 37235. E-mail: deyu.li@vanderbilt.edu

Color versions of one or more of the figures in the article can be found online at www.tandfonline.com/umte

Compared to electron transport, phonon transport has additional complexities, notably a broadband nature and a strong temperature dependence [6]. These features, combined with phonon scattering at surfaces and interfaces in nanostructured materials, lead to intriguing phenomena, which have been summarized in some excellent recent reviews [1, 2] on nanoscale thermal transport. However, these reviews are usually of a significantly broader scope and tend to be more comprehensive surveys of published literatures instead of in-depth discussions of fundamental understanding. Here, instead of a thorough review of the enormous literature on surface and interface effects in nanoscale thermal transport, we will present opinions that we have formed on phonon behavior at surfaces and interfaces and discuss how these new understandings can be used to explain interesting observations in published reports. The article starts with a brief description of phonon dynamics at surfaces and interfaces and is followed by a detailed account of how roughness, bonding strength, coupling between different boundaries, and point constriction affect thermal transport by phonons.

OVERVIEW OF THE EFFECTS OF SURFACES AND INTERFACES

If we treat phonons as particles, their transport can be described using the kinetic theory. The parameter used to measure a material's capability of conducting heat, thermal conductivity, can be derived as [7]

$$k = \frac{1}{3} C v \ell, \tag{1}$$

where k is the thermal conductivity, v is the speed of sound, and l is the phonon mean free path; that is, the average distance a phonon travels before it gets scattered. When a phonon strikes a boundary, it can transmit through it without being affected or be either specularly reflected or diffusely scattered (either forward or backward) with a random change of its propagation direction. For surfaces, only reflection or backward scattering can occur, whereas for interfaces, transmission (through either refraction or random scattering) is also possible. Scattering in the bulk can occur either through three phonon processes (normal and Umklapp) or by defects (e.g., isotopes, impurities, vacancies). In the case that the intrinsic phonon mean free path of a material (i.e., the phonon mean free path in the bulk) is comparable to or larger than the characteristic dimensions of a nanostructure or a nanostructured material, phonon–boundary interactions will affect the phonon mean free path, leading to effective thermal conductivities that can be significantly lower than the bulk value.

The probabilities of phonon reflection, transmission, and scattering at surfaces and interfaces strongly depend on the characteristics of the boundaries (e.g., roughness, bonding strength, defects) as well as the acoustic impedance of the materials in contact. The multitude of combinations of these parameters renders it difficult to precisely determine the contributions of each factor. An understanding of general mechanisms, however, can still help to achieve an understanding of phonon–boundary interactions and how these interactions affect thermal transport. A seminal review on thermal boundary resistance by Swartz and Pohl presents a comprehensive view of how different factors contribute to interfacial thermal resistance [8]. Moreover, all recent reviews of nanoscale thermal transport have significant components on surfaces and interfaces [1–6]. Instead of a comprehensive review, we therefore choose to present some of our recent understanding, based on experimental

measurements and atomistic modelling predictions, on phonon behavior at surfaces and interfaces and how it affects thermal transport in nanostructured materials.

ROUGHNESS AND SPECULARITY

Roughness plays a critical role in phonon dynamics at surfaces and interfaces because it is a key factor in the phonon specularity parameter. As mentioned above, a phonon can transmit or be reflected at thermal boundaries either specularly or diffusely, which has important implications on phonon transport. For example, reflection, no matter whether it is specular or diffuse, always contributes resistance to thermal transport in the normal direction (or cross-plane direction) of the boundary. For thermal transport parallel to the boundary (i.e., the in-plane direction), however, specular reflection does not provide resistance, whereas diffuse reflection does.

The specularity parameter, which was originally derived by Ziman to represent the percentage of phonons being specularly reflected, can be written as [9]

$$p = \exp\left(\frac{-16\pi^3\eta^2}{\lambda^2}\right), \tag{2}$$

where η is the root mean square (rms) roughness and λ is the wavelength of the energy carrier. Unless the boundary is atomically flat, Eq. (2) yields a very small specularity parameter because the thermal phonon wavelength is usually small (approximately nanometer at room temperature) and comparable to the roughness. Because it is often difficult to accurately determine the roughness of surfaces and interfaces, the specularity parameter has been widely used as a fitting parameter. Moreover, in the analysis of interface effects on the effective phonon mean free path, the specularity parameters have also been extended to transmitted phonons to account for the percentage of phonons being only refracted to all transmitted phonons, including those randomly scattered. However, a single value of the specularity parameter for all phonons, either transmitted or reflected, is typically assumed. In fact, because of the ambiguity in the specification of the specularity parameters and the fact that it is often treated simply as a fitting parameter in different studies, specularity was identified as an unsolved issue in Chen's book on nanoscale energy transport [7]. We believe that the lack of insight into the effects of surfaces and interfaces on the specularity parameter may be partly because an important understanding was missing until recently, which is that there are two different specularity parameters: one for reflected phonons and one for transmitted phonons. As such, using a single parameter to represent the specularity of both transmitted phonons and reflected phonons inevitably introduces an averaging effect, which can disguise the true transport physics.

Following the discussion of Ziman [9] on the effects of roughness on phonon specularity, we assume that phonon reflection and transmission at a thermal boundary follows Snell's law at each location. Instead of only considering reflected phonons, however, we draw both transmitted and reflected phonons at a van der Waals interface between two identical materials in Figure 1, which clearly indicates the different effects of boundary roughness on transmitted and reflected phonons. As shown in Figure 1, the boundary roughness renders a different boundary normal direction at different locations. Even though the reflection is locally specular, the overall reflection from the grain boundary is diffuse; that is, a p factor close to 0. However, for transmitted phonons, local specular transmission leads to overall specular transmission; that is, $p = 1$. This formulation can be safely extended to

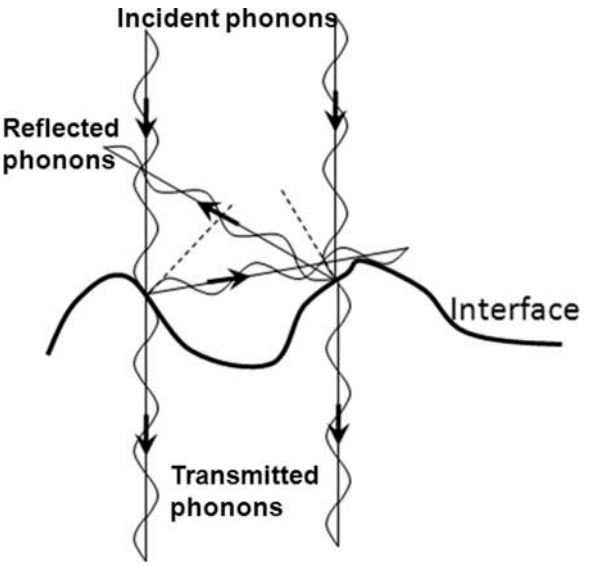

Figure 1 Schematic diagram showing phonon specularity due to interface roughness. By assuming that both sides of the interface are made of the same material and that locally both phonon reflection and transmission are specular, it can be seen that the overall reflection specularity is much less than unity, whereas the transmission specularity is unity. Even if the two sides are made of different materials—that is, refraction occurs—the specularity for transmission is still much higher than for reflection.

interfaces formed by two different materials because as long as the acoustic impedance mismatch between the two materials is not very large, the deflection of transmitted phonons from the original direction (as a result of refraction) will not be significant [8].

The view of two specularity parameters is supported by a recent study of thermal transport through boron nanoribbons [10]. Yang et al. [10] measured the in-plane thermal conductivities of single and double boron nanoribbons (two ribbons stuck together through van der Waals interactions) and found that the thermal conductivity of double ribbons could be significantly higher than the value for single ribbons. They explained this observation by assuming that a significant portion of phonons striking the van der Waals interface transmit specularly, which extends the effective phonon mean free path in the double ribbon. What is not explicitly pointed out in Yang et al.'s paper is that their explanation relies on the fact that the reflected and transmitted phonons have very different specularity parameters. This distinction is required because if the reflected phonons have the same specularity parameter as transmitted phonons, then the effective phonon mean free path in single ribbons and that in double ribbons should be the same, and no thermal conductivity enhancement could be observed for double ribbons. Therefore, the experimental observation of enhanced in-plane thermal conductivity provides solid evidence for two different specularity parameters, one for reflected and one for transmitted phonons.

The view of two specularity parameters could help to clarify some puzzles in nanoscale thermal transport involving phonon interactions with surfaces and interfaces. For example, molecular dynamics simulations of in-plane thermal conductivities of nanowires and thin films with atomically smooth surfaces have suggested relatively large specularity parameters ($p \sim 0.5$) [11]. However, experimental measurements of free-standing nanowires and thin films indicate fully diffuse scattering at the free surfaces

($p \sim 0$) [12–15]. The experimental result can be well explained by the fact that even tiny roughness, unlike the atomically flat boundaries in the modeling setup, will render a specularity parameter for reflected phonons to be essentially zero. The case is different for superlattices and multilayers, where the specularity parameter at the interfaces between layers describes the behavior of both transmitted and reflected phonons. For free-standing films, phonons are reflected at the top and bottom surfaces with a specularity parameter close to zero. At interfaces, however, depending on the ratio of reflected and transmitted phonons, the average specularity parameter could be significantly larger than zero. In fact, this is the reason why a relatively large specularity parameter is needed for modeling the in-plane thermal conductivity of superlattices, because a large portion of phonons transmit through the interface specularly [16]. In addition to superlattices and multilayers, assuming different behaviors of transmitted and reflected phonons in polycrystalline silicon helps to explain the variation in the measured thermal conductivity with different grain sizes [17].

As an outlook, we believe that Monte Carlo simulations with the assumption of two different specularity parameters at interfaces for reflected and transmitted phonons could help to clarify thermal transport through nanostructured materials with surfaces and interfaces. Note that even though this introduces two fitting parameters, it is physically more realistic and, as such, should reflect the real situation better. However, introducing more fitting parameters is usually not desirable in modeling, and caution has to be taken during the process to ensure that adopting two specularity parameters is justified. One way to avoid adding more fitting parameters is to simply assume that transmitted phonons have a specularity parameter of unity, which should be a good approximation for a high-quality interface where phonons are mainly reflected and transmitted instead of being randomly scattered by interface imperfections.

BONDING STRENGTH

Transmitted and reflected phonons make very different contributions to thermal resistance for both in-plane and cross-plane thermal transport. It is therefore important to determine the probability of transmission (i.e., the transmission coefficient) and reflection (i.e., the reflection coefficient) when a phonon strikes a boundary. Whereas for free surfaces, all striking phonons will be reflected (other than those experiencing three phonon scattering, which will be re-emitted with different frequencies), the probabilities for both transmission and reflection are significant for phonons striking an interface. Among the factors determining whether a phonon is reflected or transmitted, bonding strength is important. It is well known that phonons can scatter at weak van der Waals interfaces and, in fact, mathematical expressions exist for the phonon transmission coefficient at van der Waals interfaces [18]. These expressions have been successfully used to explain the enhanced thermal conductivity of double boron nanoribbons [10] and the interaction between supported graphene and silicon dioxide substrates [19]. As expected, these equations indicate that the phonon transmission coefficient increases with increasing bonding strength. It is not difficult to imagine that if two pieces of identical materials are joined together and the interfacial bonding strength is the same as that between two atomic planes in that material, then the phonon transmission coefficient will be unity if other scattering mechanisms at the pseudo-interface are neglected. Strong bonding strength could also facilitate phonon transmission across the interface between two different materials. However, very strong bonding strength between materials with lattice mismatch tends to introduce local strains

and defects, which could serve as efficient scattering centers to induce additional scattering events at the interface and hence decrease the phonon transmission coefficient.

Both experimental and numerical studies have been carried out to elucidate the effects of bonding strength on interfacial thermal trasport. For example, through lattice dynamics calculations, Young and Maris [20] showed that for interfaces between two lattices of different masses and spring constants, when the interfacial spring constant is lower than the spring constants of both lattices, the interfacial thermal conductance increases as the interfacial spring constant increases. In the regime where the interfacial spring constant is between the spring constants of the two lattices, the interfacial thermal conductance essentially stays the same and only reduces marginally as the interfacial spring constant further increases beyond the value for both lattices. Note that here the two lattices have the same lattice constants, so no lateral strain is introduced no matter what the interfacial spring constant is. Most molecular dynamics simulations [21, 22] suggest that the interfacial thermal conductance increases with an increase in the bonding strength between the two materials when the bonding strength is low. The conductance could saturate as the interfacial bonding strength reaches the strong bonding regime and only vary marginally with the bonding strength.

Experimental measurements of interfacial thermal conductance that systematically varied the bonding strength at the interface are limited. Hsieh et al. [23] evaluated the thermal conductance of several interfaces formed via van der Waals interactions. They found that the thermal conductance initially increases with pressure because higher pressure enhances the interactions at the interfaces. They also showed that as the pressure reaches 8 GPa, the interfacial thermal conductance only increases marginally and approaches the characteristic of strongly bonded, clean interfaces. Losego et al. [24] and O'Brien et al. [25] demonstrated that using an organic monolayer that can form strong bonds with a dielectric and a metal will significantly increase the thermal conductance at the contact and, more important, the stronger the bonding strength, the higher the thermal conductance.

Though the experimental data indicate a positive correlation between bonding strength and interfacial thermal conductance, these data were mostly obtained between materials with very different acoustic properties, such as metal and dielectrics, which have a low thermal boundary conductance without an interlayer. For two materials with similar phonon transport properties, the interfacial thermal conductance could be quite high even with a weak van der Waals interface. For example, the thermal conductance between graphene and SiO_2 (which are not similar but are both phonon-dominated materials) is determined experimentally to be $\sim$100 MW/m^2-K [26], higher than the highest value achieved at Au self-assembled monolayer–quartz interface with strong covalent bonding [23]. In this case, introducing interlayers to form strong bonding might not necessarily enhance the interfacial thermal conductance because the interlayer could effectively scatter phonons. As an outlook, similar experimental studies between two dielectric materials or two metals could provide more insights into the effects of bonding strength.

IMPLICATIONS OF PHONON REFLECTION AT FREE SURFACES

Phonon reflection plays an important role in thermal transport. Phonon scattering at free surfaces due to diffuse reflection has been regarded as the reason for significantly reduced effective thermal conductivities along the axial direction of many nanostructures [12–16]. Phonon reflection at free surfaces could also have implications beyond these

well-recognized effects. For example, if a free surface is nearby an interface, phonon reflection at the free surface could alter the thermal conductance of the interface.

Experiments by Yang et al. [27] recently showed that the normalized contact thermal conductance per unit area between two multiwalled carbon nanotubes, which is commonly expected to be size independent, is proportional to the tube diameter, which is in turn proportional to the number of tube layers. They attributed this intriguing observation to three underlying mechanisms: (1) the well-beyond 100-nm phonon mean free path along the cross-plane direction of graphite, (2) phonon reflection at free surfaces that reduces the effective phonon transmission coefficient of the contact, and (3) phonon focusing in highly anisotropic graphitic materials. Later, through molecular dynamics simulations and more detailed theoretical analyses, Liang et al. further demonstrated the effects of phonon reflection at free surfaces on the interfacial thermal conductance between a thin-film and a substrate as well as at an interface between two free surfaces [28, 29].

These studies essentially indicate a not well-recognized physical picture when phonons emitted from one object transmit through an interface/contact without being scattered and enter a nanostructure. For these transmitted phonons, if their intrinsic mean free path is larger than the characteristic size of the nanostructure, it is possible that they are not thermalized in the nanostructure (e.g., through three-phonon processes) but are reflected back into the emitting side. In this case, these reflected phonons do not contribute to energy transport from the emitting side to the nanostructure and the effective thermal conductance of the interface/contact is reduced compared to the thermal conductance of the interface/contact between the same two materials but of bulk size.

In fact, the free surface-induced size effect on the thermal conductance of an interface between two free surfaces has been observed in molecular dynamics simulations by Landry and McGaughey [30], even though they only treated this phenomenon as a size effect to be eliminated without further discussion of the underlying mechanisms. In Landry and McGaughey's [30] simulation of interfacial thermal resistance between silicon and germanium thin films, they observed that the interfacial thermal resistance decreases with increasing film thickness, as shown in Figure 2. This result can be well explained by the fact that as the films gets thicker, less phonons are reflected back into the emitting side, leading to an enhancement of the interfacial thermal conductance. It is worth noting that we are discussing an interesting regime of phonon transport. Though it is widely accepted that phonon scattering poses resistance to energy transport, in cases where free surfaces reflect phonons back to their emitting side, enhancing phonon scattering within the receiving side will promote thermal transport across the interface.

In addition to the effects on thermal conductance of nearby interfaces, we believe that phonon reflection at free surfaces plays an important role in one scheme of nonequilibrium molecular dynamics (NEMD) simulations for thermal conductivity prediction. One common scheme of NEMD adopts a simulation domain as shown in Figure 3a, in which a sample region is sandwiched by a heat source and a heat sink. The heat source/sink either has free surfaces or is bounded by a fixed layer. We note that the effects of free surfaces and fixed layers on incoming phonons are the same; that is, they reflect all incident phonons other than those experiencing three-phonon scattering at the outmost layer of the heat source/sink. The important effects of phonon reflection at the boundary of heat source/sink, which are critical for the validity of this NEMD scheme, are as follows.

First, the phonon reflection at these boundaries helps to establish local thermal equilibrium within the sample domain. In NEMD simulations, because of the limited domain size, it is common that the intrinsic phonon mean free path is larger than the sample domain

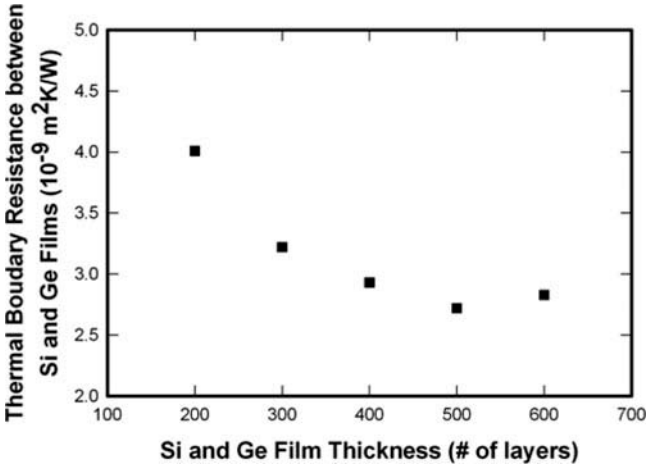

Figure 2 Molecular dynamics simulation results of the interfacial thermal resistance between Si and Ge films as a function of the thickness of the films. The data is from Landry and McGaughey [30]. It is clear that the interfacial thermal resistance increases as the film thickness reduces, which we attribute to enhanced phonon reflection from the free boundaries as the film thicknesses gets smaller.

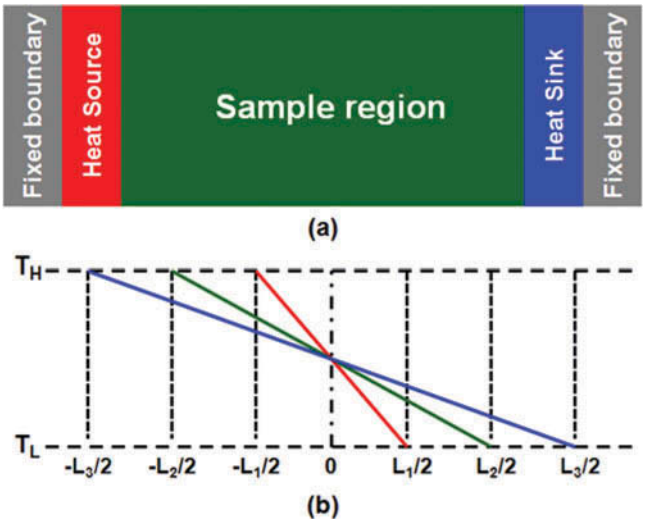

Figure 3 (a) Schematic diagram of common NEMD simulation domain for predicting the thermal conductivity of a thin film. (b) With an imposed heat flux through the film, a linear temperature profile is formed in the sample domain. If the intrinsic phonon mean free path is much larger than the film thickness, the temperature gradient increases as the film thickness reduces (L_1, L_2, L_3 denote the length of different simulation domains). For a given heat flux, this increase is required to realize a lower thermal conductivity for thinner films.

size, in which case phonon transport in the sample domain is partially ballistic. In fact, if the phonon mean free path is much larger than the domain length, phonon transport in the sample domain is mainly ballistic. The most thoroughly discussed case for ballistic transport is with perfectly absorbing/emitting boundary conditions, in which at any position, the phonons take two different distributions of the heat source and heat sink, as shown in

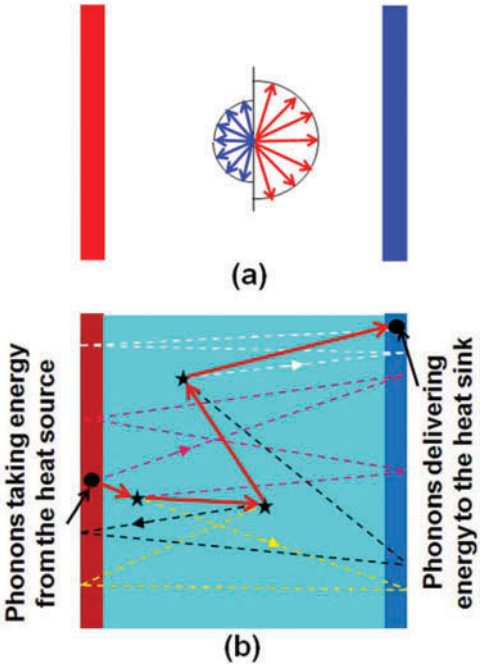

Figure 4 Effects of different boundary conditions on phonon transport in a thin film when the intrinsic phonon mean free path is much larger than the film thickness. (a) Perfectly absorbing/emitting heat source/sink, which leads to a nonequilibrium phonon distribution at all locations in the film. (b) If the heat source/sink is part of the film and not perfectly absorbing/emitting, then phonons will travel back and forth through the film before depositing energy in the heat source/sink. In this case, the phonons arriving at each point are from everywhere in the film and take a Boltzmann distribution. The energy carried by phonons follows a diffusive zigzag path from the heat source to the heat sink.

Figure 4a. In this case, there is no thermal equilibrium in the sample domain and no equilibrium temperature can be defined. Note that in this case, time-averaging will not help phonons at any location to achieve the Boltzmann distribution, a characteristic for thermal equilibrium. However, such behavior is not the case in NEMD simulations, as shown in a benchmark study by Lukes et al. [31], where statistics showed that the velocity distribution of atoms follows the Boltzmann distribution, indicating that the time-averaged velocities reach thermal equilibrium.

We believe that this equilibrium is reached because of phonon reflection at the boundaries. As shown in Figure 4b, due to the fact that the phonon mean free path is larger than the film thickness, phonons emitted from the heat source will travel ballistically to the heat sink. However, other than those thermalized in the heat sink, phonons will be reflected back into the system and, after traveling back and forth, eventually experience a three-phonon scattering event somewhere. The re-emitted phonons will carry the information of where these scattering events occur. The process is repeated throughout the long time of the simulation (typically many nanoseconds). Therefore, at each location, the phonons present are not just from the heat source and heat sink but from the entire simulation domain. As such, the time-averaged phonon distribution will, at least approximately, take the Boltzmann distribution, allowing for definition of a temperature representing local thermal equilibrium.

One might argue that the velocity rescaling or thermostating in the heat source/sink to add/remove heat should be an effective phonon scattering mechanism and that the NEMD simulation should in fact resemble the case of perfectly absorbing/emitting boundary conditions. We believe that this interpretation is not the case because if it were, clear temperature jumps would occur at the boundaries between the heat source/sink and the sample domain. No such sudden temperature jump exists in NEMD simulations and the temperature distribution has a continuous profile [31, 32]. In addition, NEMD simulations of thermal transport between two graphite thin films with a slit contact indicate that no matter whether the heat source/sink is taken as the whole hot/cold ribbons or only placed at the edge of the ribbons, the result is the same. This observation will only be the case if the phonon mean free path is long and not significantly affected by velocity rescaling [27]. Now if velocity rescaling is extremely effective in phonon scattering, then when the whole ribbons are taken as heat source/sink, phonons will be scattered everywhere and cannot possess a long mean free path.

In addition to helping to establish local thermal equilibrium, phonon reflection from free surfaces or fixed boundaries underlies the thermal conductivity calculation of thin films or nanostructures with a size less than the intrinsic phonon mean free path. It is well known that the effective thermal conductivity of a thin film along the cross-plane direction can be significantly reduced compared to the bulk value when the thickness of the thin film is less than the phonon mean free path. In this regime, the effective thermal conductivity increases with the film thickness and NEMD simulations correctly reflect this trend [31]. A common scheme in the NEMD simulation is to impose a certain heat flux and after the system reaches thermal equilibrium, solve for the linear temperature profile in the sample region, and derive the thermal conductivity based on the imposed heat flux and the resulting temperature gradient. To obtain the correct dependence of thermal conductivity on the film thickness—that is, smaller thermal conductivity for thinner films—the temperature gradient needs to be larger for thinner films, as shown in Figure 3b. This behavior cannot be realized if the boundaries are perfectly absorbing/emitting and phonons only pass through the thin film once. Note that when the film thickness is much less than the phonon mean free path, the thermal resistance of the film is approximately constant and, as such, the temperature drop across the film is nearly the same under a given heat flux.

Now the question is how the temperature gradient can be larger for thinner films under the condition that the phonon mean free path is much larger than the film thickness—or, equivalently, how can the sample region, instead of the thermal boundaries, contribute the dominant thermal resistance. To answer this, we consider the phonon transport picture as described in Figure 4b, which indicates that whereas phonon transport is ballistic in the thin film, the energy carried by phonons goes through a zigzag path from the heat source to the heat sink, which is the signature of diffusive energy transport. As such, we conclude that due to phonon reflection at free surfaces or fixed boundaries, energy transport in NEMD simulations for thin films of thickness less than the bulk phonon mean free path is diffusive even though phonon transport is dominantly ballistic; that is, there exists an interesting regime where phonon transport is ballistic yet the energy transport is diffusive. Note that this is a result of combined effects of phonon reflection and that phonon transport is never fully ballistic. No matter how small it is, there is always some finite probability for three-phonon scattering events to occur in the film, which, combined with phonon reflection from the free surfaces, leads to a situation where three-phonon scattering processes in the thin film dominate thermal transport in a ballistic phonon transport regime.

As an outlook, phonon reflection has deep implications. Though the consequences are more prominent at free surfaces, similar effects should exist for phonons reflected at

interfaces. In this case, however, phonon transmission and additional phonon scattering from interface imperfections compete with phonon reflection, resulting in more complex phenomena. Analyses of phonon transport through multilayer and superlattices with better understanding of the phonon reflection effects should shed more lights in these situations.

COHERENCE

Recently, the wave nature of phonons has attracted considerable attention and the effects of phonon coherence on thermal transport have become a topic of significant interest [33]. Phonon–boundary interactions could play a significant role in coherent phonon transport and are responsible for some very interesting phenomena, such as the minimum cross-plane thermal conductivity of superlattices.

Physically, coherence means that two waves retain their phase information and their capability to interfere. Therefore, ballistic phonons can be denoted as coherent phonons because they preserve their phase information. In this case, even though the phonons are coherent, their contributions to thermal transport can be explained with the more straightforward ballistic transport picture.

The wave nature of phonons was first experimentally demonstrated via measurements of the transmission coefficient of quasi-monochromatic acoustic phonons through GaAs/AlGaAs superlattices using superconducting tunnel junctions [34]. It was shown that the transmission coefficient for certain phonon frequency is significantly reduced due to the formation of stop bands. More recently, confinement of acoustic phonon modes using a phonon cavity formed by two GaAs/AlAs superlattices as the reflection layers further confirmed the possibility of using coherence to manipulate phonon transport [35].

The effect of coherence on thermal transport for a broad spectrum of phonons has been identified in superlattices through the measurement of a minimum thermal conductivity as the period length of the superlattices increases from a value less than the intrinsic phonon mean free paths of each constituent material. Venkatasubramanian [36] first reported that the lattice thermal conductivity of Bi_2Te_3/Sb_2Te_3 achieved a minimum value at a period length of around 60 Å. Later, it was shown that this minimum thermal conductivity could lead to a record-high thermoelectric figure-of-merit for well-designed superlattices [37]. Simkin and Mahan [38] used a simple lattice dynamics model to explain the observation and suggested that the minimum thermal conductivity is due to the formation of minibands in the phonon dispersion. The minimum thermal conductivity was not observed in studies of Si/Ge superlattices until a report by Chakraborty et al. using strain symmetrised Si/Ge superlattices [39]. To explain the fact that most experimental measurements do not show a minimum thermal conductivity, Chen et al. conducted molecular dynamics simulations to explore the effects of various parameters on thermal transport in superlattices [40]. Their results show that the minimum thermal conductivity can be observed only when phonons retain their coherence upon reflection from the interfaces in superlattices, which helps to form the minibands. However, phonon coherence can be easily destroyed by interfacial imperfections such as defects and dislocations. In fact, with a 4% lattice constant mismatch between the alternating layers in the model superlattices, the minimum thermal conductivity disappeared. More recently, to provide more solid experimental evidence of phonon coherence in superlattices, Ravichandran et al. [41] prepared $SrTiO_3/CaTiO_3$ and $SrTiO_3/BaTiO_3$ superlattices. Their high-resolution transmission electron microscopy micrographs indicate atomically sharp interfaces that are conducive for the reflected phonons to retain their coherence. Their measurements demonstrated that when

the period length is less than the intrinsic phonon mean free path, the thermal conductivity decreases with increasing period length, which is a result of miniband formation.

In interpreting superlattice thermal conductivity data, a key decision is how to specify the phonon modes. The superlattice period defines its unit cell and the true superlattice phonon modes. Due to the large superlattice lattice constant, these phonon modes have a Brillouin zone that is smaller than that of the constituent bulk materials. It is in this reduced Brillouin zone that the minibands exist. This description of the superlattice, where there is no interface scattering, is always valid when phonon coherence is preserved in the superlattices. As the superlattice period is increased, some phonon modes can be thought of as having wavelengths that are smaller than the period, such that they will see a bulk-like environment in a given layer. These phonons can be modeled as bulk-like modes that scatter at the internal interfaces. As the superlattice period increases, more of the modes can be treated with this approximation. It is the transition from a description of true superlattice phonon modes to bulk-like phonon modes that leads to the existence of the thermal conductivity minimum.

As an outlook, though phonon coherence effects are confirmed through the observation of a minimum cross-plane thermal conductivity of superlattices, it is interesting to consider what the effects should be to in-plane transport. In addition, one can ask whether it is possible to use a combination of superlattices with different period lengths to filter phonons from across the spectrum to further reduce the cross-plane thermal transport. Finally, it is worth noting that though phonon coherence could lead to intriguing phenomena, phonon transport can still be viewed with the particle picture after the effects of phonon coherence are considered with a modified phonon dispersion.

PHONON TRANSPORT AT NANOSCALE CONTACTS

Phonon transport through nanoscale contacts is important in a broad spectrum of applications. Examples include tip–surface contacts in scanning thermal microscopy [42], sample–heat source/sink contacts in thermal bridge methods for individual nanostructure thermal property characterization [43–46], and point contacts between carbon nanotubes or other nanowires in their nanocomposites [27, 47, 48] or with substrates in thermal interface materials [49].

The thermal resistance of a nanoscale contact depends on the materials in contact, the strength of the van der Waals interactions at the contacts, the actual contact area, the ratio of the characteristic dimensions of the contact and the objects in contact, and the ratio of the characteristic dimension of the contact and the intrinsic phonon mean free paths of the materials in contact. As a result, the thermal resistance of a nanoscale contact is an extremely complex issue and it is often difficult to resolve the contributions from these different factors. Because an interface between two objects exists at the contact, essentially all of the factors we discussed in the previous sections about phonon transport through interfaces play an important role in the contact thermal resistance. In addition, because nanoscale contacts usually represent a geometrical constriction, the resistance due to size confinement plays a significant role. In fact, the total thermal resistance is usually dominated by the size confinement of the contact. It is therefore important to have an accurate estimation of the contact area, which is, unfortunately, usually difficult to evaluate. Various models have been developed in the solid mechanics community to predict the contact area between two solid objects [50], which commonly involve the Young's moduli of the materials in contact and their shapes and surface morphologies. We note that the Young's moduli

of a nanostructure can be significantly different from that of the bulk [51] and that models are usually developed only for objects of regular shapes, rendering accurate estimation of the contact area a daunting challenge. Moreover, these models have been developed based on well-defined interaction potentials between the objects in contact, which might not be the case in reality. In fact, we have observed from our experiments [10] that even though no difference at the contact can be seen under an electron microscope, the contact from a wet process, during which surface tension helps to pull a nanostructure (e.g., a boron nanoribbon) to a suspended membrane, dramatically reduces the contact resistance.

Since the 1950s, the effect of a geometrical constriction on contact thermal resistance has attracted attention. Depending on the ratio of the characteristic length of the contact area and the bulk phonon mean free paths of the two materials in contact, two models—that is, the diffusive constriction resistance and the ballistic contact resistance (also referred to as the Sharvin resistance)—have been developed. Cooper et al. [52] first reported the detailed derivation of the diffusive constriction resistance by solving the heat diffusion equation with proper boundary conditions. The well-known form of diffusive constriction resistance—that is, that of a point contact between two semi-infinite objects of identical materials—is written as

$$R_{c,d} = \frac{1}{2ka}, \tag{3}$$

where k is the thermal conductivity of the semi-infinite objects and a is the characteristic size (radius) of the contact. This expression is only strictly applicable for a very ideal case and it can lead to significant error as the situation gets more complex. For example, if the two materials are different, the thermal conductivity needs to be taken as $1/k = 1/2 \times (1/k_1 + 1/k_2)$. Moreover, if the contact size is not much smaller than the size of the objects in contact, which is a likely scenario for nanostructures in contact, the expression needs to be modified significantly [52].

One important understanding that has emerged from recent nanoscale thermal transport studies is that the phonon mean free path estimated using Eq. (1) is usually considerably less than the actual value because of the complication from optical phonons as well as the broadband nature of acoustic phonons. This has been the case for Si [53], graphite in the cross-plane direction [54, 55], etc. As such, for nanostructures in contact, the characteristic size of the contact is usually much less than the phonon mean free path, which leads to a significant contribution from the Sharvin resistance, expressed as [56]

$$R_{c,b} = \frac{4\ell}{3kA_c}, \tag{4}$$

where A_C is the contact area and ℓ is the phonon mean free path. The detailed derivation of Eq. (4) can be found in Chen's book [7]. A simple way of interpreting the Sharvin resistance is that it is equal to the resistance of a column with the contact area as the bottom and a height of the phonon mean free path. This interpretation results from that each phonon pointing to the contact area can be replaced with an equivalent phonon within the column through specular reflection at the column boundary, as shown in Figure 5. This equivalence enables analysis using Eq. (4) for some highly anisotropic materials such as graphite or carbon nanotubes, in which phonon focusing renders highly anistropic phonon transport different from the picture from which Eq. (4) is derived. (Note that strict mathematical

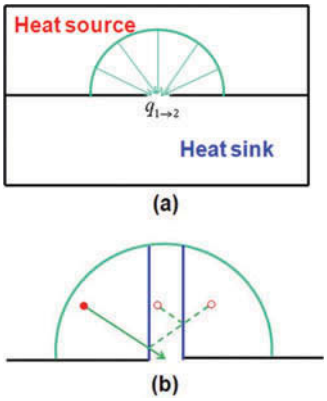

Figure 5 (a) Schematic of Sharvin resistance. Within the hemisphere of the phonon mean free path, only phonons pointing to the small constriction can pass through. (b) Equivalence of Sharvin resistance to the resistance of a column with the constriction as the bottom and the phonon mean free path as the height. This is because each phonon pointing to the constriction corresponds to a phonon with the column through specular reflection at the column boundary. Note that the phonon density is uniform within the hemisphere.

derivation of the equivalence still needs to be done to prove the conceptual speculation based on Figure 5 for highly anisotropic materials.)

Note that Eqs. (3) and (4) only consider the effects of geometrical constriction, which plays a dominant role in the total resistance of a small nanoscale contact. However, contributions from other factors could be important, which can be most conveniently analyzed through examining the normalized contact thermal conductance or resistance per unit area. The effects of all factors discussed in the previous sections should be reflected in the normalized conductance or resistance. For example, through analysis of the normalized conductance between multiwalled carbon nanotubes, a recent study elucidated the important contribution of phonon reflection from the innermost tube layers [27]. In fact, in a study of contact thermal conductance between a silicon tip and a substrate by Pettes and Shi [57], a modified formula of Eq. (4) with a transmission coefficient added to the denominator, could reasonably explain the experimental data if the maximum contact area is assumed. It is also worth noting that all discussions so far are applicable only to thermal transport by phonons, without potential complications from radiation or conduction/convection from air or other fluids at the contact.

Because of the great complexities involved in phonon transport through nanoscale contacts, limited experimental data are available and not enough attention has been devoted to fully dissect the potential contributions from all different factors. If contact thermal resistance is not carefully considered in many thermal measurements of nanostructures, however, it might lead to erroneous explanations of the experimental results. Therefore, it is important to explicitly examine the contribution of nanoscale contacts in these experiments.

SUMMARY

We presented our opinions on phonon dynamics at thermal boundaries and nanoscale contacts and their implications. These opinions are based on both our recent experimental/numerical studies and relevant publications from others; however, this is not

intended to be a comprehensive review. Some opinions, such as the two specularity parameters at interfaces and the implications of phonon reflection at free surfaces, have not been discussed in literature. We also offer some outlook and potential topics for future studies.

ACKNOWLEDGMENTS

D. Li acknowledges the very helpful discussions with Drs. Yunfei Chen, Chris Dames, Ravi Prasher, Li Shi, and Juekuan Yang.

FUNDING

D. Li acknowledges the support from the U.S. National Science Foundation (Grant No. 0800306, 1067213, 1308550, and 1403456). A. McGaughey acknowledges financial support from the U.S. National Science Foundation (Grant No. 1006480).

REFERENCES

1. D.G. Cahill, W.K. Ford, K.E. Goodson, G.D. Mahan, A. Majumdar, H.J. Maris, R. Merlin, and S.R. Phillpot, Nanoscale Thermal Transport, *Journal of Applied Physics*, Vol. 93, p. 793–818, 2003.
2. D.G. Cahill, P.V. Braun, G. Chen, D.R. Clarke, S. Fan, K.E. Goodson, P. Keblinski, W.P. King, G.D. Mahan, A. Majumdar, H.J. Maris, S.R. Phillpot, E. Pop, and L. Shi, Nanoscale Thermal Transport II. 2003–2012, *Applied Physics Review*, Vol. 1, p. 011305, 2014.
3. E. Pop, Energy Dissipation and Transport in Nanoscale Devices, *Nano Research*, Vol. 3, pp. 147–169, 2010.
4. G. Chen and A. Shakouri, Heat Transfer in Nanostructures for Solid-State Energy Conversion, *Journal of Heat Transfer*, Vol. 124, pp. 242–252, 2001.
5. Z. Han and A. Fina, Thermal Conductivity of Carbon Nanotubes and Their Polymer Nanocomposites: A Review, *Progress in Polymer Science*, Vol. 36, pp. 914–944, 2011.
6. D. Li, S. Huxtable, A. Abramson, and A. Majumdar, Thermal Transport in Nanostructured Solid State Cooling Devices, *Journal of Heat Transfer*, Vol. 127, pp. 108–114, 2005.
7. G. Chen, *Nanoscale Energy Transport and Conversion: A Parallel Treatment of Electronics, Molecules, Phonons, and Photons*, Oxford University Press, New York, 2005.
8. E.T. Swartz and R.O. Pohl, Thermal Boundary Resistance, *Reviews of Modern Physics*, Vol. 61, p. 605–668, 1989.
9. J.M. Ziman, *Electrons and Phonons: The Theory of Transport Phenomena in Solids*, Oxford University Press, Oxford, UK, 1960.
10. J. Yang, Y. Yang, S.W. Waltermire, X. Wu, H. Zhang, T. Gutu, Y. Jiang, Y. Chen, A.A. Zinn, R. Prasher, T.T. Xu, and D. Li, Enhanced and Switchable Nanoscale Thermal Conduction Due to van der Waals Interfaces, *Nature Nanotechnology*, Vol. 7, pp. 91–95, 2012.
11. S.G. Volz and G. Chen, Molecular Dynamics Simulation of Thermal Conductivity of Silicon Nanowires, *Applied Physics Letters*, Vol. 75, pp. 2056–2058, 1999.
12. D. Li, Y. Wu, P. Kim, L. Shi, P. Yang, and A. Majumdar, Thermal Conductivity of Individual Silicon Nanowires, *Applied Physics Letters*, Vol. 83, pp. 2934–2936, 2003.
13. N. Mingo, L. Yang, D. Li, and A. Majumdar, Predicting the Thermal Conductivity of Si and Ge Nanowires, *Nano Letteres*, Vol. 3, pp. 1713–1716, 2003.
14. D. Li, Y. Wu, R. Fan, P. Yang, and A. Majumdar, Thermal Conductivity of Si/SiGe Superlattice Nanowires, *Applied Physics Letters*, Vol. 83, pp. 3186–3188, 2003.
15. C. Dames and G. Chen, Theoretical Phonon Thermal Conductivity of Si/Ge Superlattice Nanowires, *Journal of Applied Physics*, Vol. 95, pp. 682–693, 2004.

16. G. Chen, Size and Interface Effects on Thermal Conductivity of Superlattices and Periodic Thin-Film Structures, *Journal of Heat Transfer*, Vol. 119, pp. 220–229, 1997.
17. Z. Wang, J.E. Alaniz, W. Jang, J.E. Garay, and C. Dames, Thermal Conductivity of Nanocrystalline Silicon: Importance of Grain Size and Frequency-Dependent Mean Free Paths, *Nano Letters*, Vol. 11, pp. 2206–2213, 2011.
18. R. Prasher, Acoustic Mismatch Model for Thermal Contact Resistance of van der Waals Contacts, *Applied Physics Letters*, Vol. 94, p. 041905, 2009.
19. J.-H. Seol, I. Jo, A.L. Moore, L. Lindsay, Z.H. Aitken, M.T. Pettes, X. Li, Z. Yao, R. Huang, D. Broido, N. Mingo, R.S. Ruoff, and L. Shi, Two-Dimensional Phonon Transport in Supported Graphene, *Science*, Vol. 328, pp. 213–216, 2010.
20. D.A. Young and H.J. Maris, Lattice-Dynamical Calculation of the Kapitza Resistance between FCC Lattices, *Physical Review B*, Vol. 40, pp. 3685–3693, 1989.
21. J.C. Duda, T.S. English, E.S. Piekos, W.A. Soffa, L.V. Zhigilei, and P.E. Hopkins, Implications of Cross-Species Interactions on the Temperature Dependence of Kapitza Conductance. *Physical Review B*, Vol. 84, p. 193301, 2011.
22. M. Hu, P. Keblinski, and P.K. Schelling, Kapitza Conductance of Silicon–Amorphous Polyethylene Interfaces by Molecular Dynamics Simulations, *Physical Review B*, Vol. 79, p. 104305, 2009.
23. W.-P. Hsieh, A.S. Lyons, E. Pop, P. Keblinski, and D.G. Cahill, Pressure Tuning of the Thermal Conductance of Weak Interfaces, *Physical Review B*, Vol. 84, p. 184107, 2011.
24. M.D. Losego, M.E. Grady, N.R. Sottos, D.G. Cahill, and P.V. Braun, Effects of Chemical Bonding on Heat Transport across Interfaces, *Nature Materials*, Vol. 11, pp. 502–506, 2012.
25. P.J. O'Brien, S. Shenogin, J. Liu, P.K. Chow, D. Laurencin, P.H. Mutin, M. Yamaguchi, P. Keblinski, and G. Ramanath, Bonding-Induced Thermal Conductance Enhancement at Inorganic Heterointerfaces Using Nanomolecular Monolayers, *Nature Materials*, Vol. 12, pp. 118–122, 2013.
26. Z. Chen, W. Jang, W. Bao, C.N. Lau, and C. Dames, Thermal Contact Resistance between Graphene and Silicon Dioxide, *Applied Physics Letters*, Vol. 95, p. 161910, 2009.
27. J. Yang, M. Shen, Y. Yang, W.J. Evans, Z. Wei, W. Chen, A. A. Zinn, Y. Chen, R. Prasher, T.T. Xu, P. Keblinski, and D. Li, Phonon Transport through Point Contacts between Graphitic Nanomaterials, *Physical Review Letters*, Vol. 112, p. 205901, 2014.
28. Z. Liang, K. Sasikumar, and P. Keblinski, Thermal Transport across a Substrate–Thin-Film Interface: Effects of Film Thickness and Surface Roughness, *Physical Review Letters*, Vol. 113, p. 065901, 2014.
29. Z. Liang and P. Keblinski, Finite-Size Effects on Molecular Dynamics Interfacial Thermal-Resistance Predictions, *Physical Review B*, Vol. 90, p. 075411, 2014.
30. E.S. Landry and A.J.H. McGaughey, Thermal Boundary Resistance Predictions from Molecular Dynamics Simulations and Theoretical Calculations, *Physical Review B*, Vol. 80, p. 165304, 2009.
31. J.R. Lukes, D. Li, X.-G. Liang, and C.-L. Tien, Molecular Dynamics Study of Solid Thin-Film Thermal Conductivity, *Journal of Heat Transfer*, Vol. 122, pp. 536–543, 2000.
32. E.S. Landry and A.J.H. McGaughey, Effect of Film Thickness on the Thermal Resistance of Confined Semiconductor Thin Films, *Applied Physics Letters*, Vol. 107, p. 013521, 2010.
33. M.N. Luckyanova, J. Garg, K. Esfarjani, A. Jandl, M.T. Bulsara, A.J. Schmidt, A.J. Minnich, S. Chen, M.S. Dresselhaus, Z. Ren, E.A. Fitzgerald, and G. Chen, Coherent Phonon Heat Conduction in Superlattices, *Science*, Vol. 338, pp. 936–939, 2012.
34. V. Narayanmurti, H.L. Störmer, M.A. Chin, A.C. Gossard, and W. Wiegmann, Selective Transmission of High-Frequency Phonons by a Superlattice: The Dielectric Phonon Filter, *Physical Review Letters*, Vol. 43, pp. 2012–2016, 1979.
35. M. Trigo, A. Bruchhausen, A. Fainstein, B. Jusserand, and V. Thierry-Mieg, Confinement of Acoustic Vibrations in a Semiconductor Planar Phonon Cavity, *Physical Review Letters*, Vol. 89, p. 227402, 2002.

36. R. Venkatasubramanian, Lattice Thermal Conductivity Reduction and Phonon Localization Behavior in Superlattice Structures, *Physical Review B*, Vol. 61, pp. 3091–3097, 2000.
37. R. Venkatasubramanian, E. Siivola, T. Colpitts, and B. O'Quinn, Thin-Film Thermoelectric Devices with High Room-Temperature Figures of Merit, *Nature*, Vol. 413, pp. 597–602, 2001.
38. M.V. Simkin and G.D. Mahan, Minimum Thermal Conductivity of Superlattices, *Physical Review Letters*, Vol. 84, pp. 927–930, 2000.
39. S. Chakraborty, C.A. Kleint, A. Heinrich, C.M. Schneider, J. Schumann, M. Falke, and S. Teichert, Thermal Conductivity in Strain Symmetrized Si/Ge Superlattices on Si(111), *Applied Physics Letters*, Vol. 83, pp. 4184–4186, 2003.
40. Y. Chen, D. Li, J.R. Lukes, Z. Ni, and M. Chen, Minimum Thermal Conductivity of Superlattices from Molecular Dynamics, *Physical Review B*, Vol. 72, p. 174302, 2005.
41. J. Ravichandran, A.K. Yadav, R. Cheaito, P.B. Rossen, A. Soukiassian, S.J. Suresha, J.C. Duda, B.M. Foley, C.-H. Lee, Y. Zhu, A.W. Lichtenberger, J.E. Moore, D.A. Muller, D.G. Schlom, P.E. Hopkins, A. Majumdar, R. Ramesh, and M.A. Zurbuchen, Crossover from Incoherent to Coherent Phonon Scattering in Epitaxial Oxide Superlattices, *Nature Materials*, Vol. 13, pp. 168–172, 2014.
42. L. Shi and A. Majumdar, Thermal Transport Mechanisms at Nanoscale Point Contacts, *Journal of Heat Transfer*, Vol. 124, pp. 329–337, 2002.
43. L. Shi, D. Li, C. Yu, W. Jang, Z. Yao, and A. Majumdar, Measuring Thermal and Thermoelectric Properties of One-Dimensional Nanostructures Using a Microfabricated Device, *Journal of Heat Transfer*, Vol. 125, pp. 881–888, 2003.
44. J. Yang, Y. Yang, S.W. Waltermire, T. Gutu, A.A. Zinn, T.T. Xu, Y. Chen, and D. Li, Measurement of the Intrinsic Thermal Conductivity of a Multiwalled Carbon Nanotube and Its Contact Thermal Resistance with the Substrate, *Small*, Vol. 7, pp. 2334–2340, 2011.
45. R. Prasher, Thermal Boundary Resistance and Thermal Conductivity of Multiwalled Carbon Nanotubes, *Physical Review B*, Vol. 77, p. 075424, 2008.
46. K. Hippalgaonkar, B.L. Huang, R.K. Chen, K. Sawyer, P. Ercius, and A. Majumdar, Fabrication of Microdevices with Integrated Nanowires for Investigating Low-Dimensional Phonon Transport, *Nano Letters*, Vol. 10, pp. 4341–4348, 2010.
47. F. Zhou, A. Persson, L. Samuelson, H. Linke, and L. Shi, Thermal Resistance of a Nanoscale Point Contact to an Indium Arsenide Nanowire, *Applied Physics Letters*, Vol. 99, p. 063110, 2011.
48. R. Prasher, X.J. Hu, Y. Chalopin, N. Mingo, K. Lofgreen, S. Volz, F. Cleri, and P. Keblinski, Turning Carbon Nanotubes from Exceptional Heat Conductors into Insulators, *Physical Review Letters*, Vol. 102, p. 105901, 2009.
49. B.A. Cola, X. Xu, and T.S. Fisher, Increased Real Contact in Thermal Interfaces: A Carbon Nanotube/Foil Material, *Applied Physics Letters*, Vol. 90, p. 093513, 2007.
50. K.L. Johnson, *Contact Mechanics*, Cambridge University Press, Cambridge, UK, 1985.
51. Y. Zhu, F. Xu, Q. Qin, W.Y. Fung, and W. Lu, Mechanical Properties of Vapor–Liquid–Solid Synthesized Silicon Nanowires, *Nano Letters*, Vol. 9, pp. 3934–3939, 2009.
52. M.G. Cooper, B.B. Mikic, and M.M. Yovanovich, Thermal Contact Conductance, *International Journal of Heat and Mass Transfer*, Vol. 12, pp. 279–300, 1969.
53. Y.S. Ju and K.E. Goodson, Phonon Scattering in Silicon Films with Thickness of Order 100 nm, *Applied Physics Letters*, Vol. 74, pp. 3005–3007, 1999.
54. Z. Wei, J. Yang, W. Chen, K. Bi, D. Li, and Y. Chen, Phonon Mean Free Path of Graphite along the *c*-Axis, *Applied Physics Letters*, Vol. 104, p. 081903, 2014.
55. Q. Fu, J. Yang, Y. Chen, D. Li, and D. Xu, Experimental Evidence of Very Long Intrinsic Phonon Mean Free Path along the c-Axis of Graphite, *Applied Physics Letters*, Vol. 106, p. 031905, 2015.
56. R. Prasher, Predicting the Thermal Resistance of Nanosized Constrictions, *Nano Letters*, Vol. 5, pp. 2155–2159, 2005.
57. M.T. Pettes and L. Shi, A Reexamination of Phonon Transport through a Nanoscale Point Contact in Vacuum, *Journal of Heat Transfer*, Vol. 136, p. 0032401, 2014.